Journal of Alloys and Compounds 526 (2012) 31–38

Contents lists available at SciVerse ScienceDirect

Journal of Alloys and Compounds

journal homepage: www.elsevier.com/locate/jallcom

Phase separation and thermoelectric properties of the $Pb_{0.25}Sn_{0.25}Ge_{0.5}Te$ compound

Y. Rosenberg, Y. Gelbstein, M.P. Dariel*

Department of Materials Engineering, Ben-Gurion University of the Negev, Beer-Sheva, Israel

ARTICLE INFO

Article history:
Received 10 January 2012
Received in revised form 9 February 2012
Accepted 13 February 2012
Available online xxx

Keywords:
Discontinuous precipitation
Chalcogenide compounds
Cellular nanostructure
Phase separation
Aging
Thermoelectric properties

ABSTRACT

The $Pb_{0.25}Sn_{0.25}Ge_{0.5}Te$ compound is a promising p-type thermoelectric material. It is single phased at elevated temperature and undergoes upon cooling an allotropic transformation from the cubic Ge_β, to the rhombohedral Ge_α structure. In addition, a phase separation takes place in the course of aging treatments within the miscibility gap at lower temperature. The phase separation in this pseudo-ternary system takes place by a discontinuous precipitation process, giving rise to a heterogeneously nucleated coupled structure of Pb- and Ge-rich lamellae, with 10^2 nm to 2 μm wide spacing. The presence of Sn atoms in the structure tends to suppress the spinodal decomposition and is characteristic of the low Sn content compounds. The phase separation by discontinuous precipitation follows the Johnson–Mehl–Avrami kinetics. In the course of further lengthy aging treatments at 390 °C, the microstructure consists of spheroidized Ge-rich precipitates in a Pb-rich telluride matrix. The thermoelectric transport properties undergo significant changes in the initial stages of the phase separation process, leading to a stable and relatively elevated figure of merit, $ZT = 0.95 \pm 0.07$ at 400 °C.

1. Introduction

Thermoelectric materials have elicited substantial interest over the past decade on the background of the quest for clean and renewable energy. The main obstacle to the wide spread use of these materials is their low conversion efficiency of thermal to usable electric energy. Worldwide efforts are being made in order to develop efficient materials by synthesizing new ones and by improving the efficiency of the known ones. Efficiency can be improved by appropriate composition changes e.g. alloying and doping or by engineering the microstructure. The figure of merit is a measure of the efficiency of thermoelectric materials and is inversely proportional to the thermal conductivity. As shown a decade ago roughly, the thermal conductivity can be drastically reduced in nano-structured materials, in which phonon scattering interfaces are more closely spaced than the mean free path of phonons.

Nano-structures, which display a high interface density, can be prepared with relative ease by fast cooling low dimensional, 1D or 2D materials from the gaseous or the liquid phase, on account of easy heat evacuation. A low dimensional material has the intrinsic drawback of being of use only for low power applications. For most applications nano-structured materials can be manufactured by either the 'bottom up' or the 'top down' approach. The former requires the consolidation of initial nano-particles in a bulk material, a process that entails some elevated temperature exposure. The latter relies on thermodynamically driven processes that generate by precipitation in the solid state or by phase separation from the liquid or solid, nano or submicron scaled structures.

Lead based chalcogenides are among the most popular thermoelectric materials for energy conversion in the intermediate, 200–600 °C temperature range. Various quasi-binary and quasi-ternary compounds in this family have been the subject to extensive investigations aimed at optimizing the composition and the microstructure. The possibility of enhancing the thermoelectric figure of merit ZT by multiplying the density of interfaces and thereby decreasing the thermal conductivity has prompted many studies in a variety of material systems. Snyder and co-workers [1,2] have carried out an extensive investigation of the submicron phase separation that takes place in Pb(Te,Sb) pseudo-binary compounds, following cooling from the melt and a subsequent solid phase Widmanstatten-type precipitation reaction. These authors also determined the change of precipitate density as a function of annealing time. The presence of a nano-structured material that leads to a reduced thermal conductivity does not ensure, however, its viability for thermoelectric applications. Such applications most often require the material to perform continuously at temperatures that may affect the nano-structure. Surface free energy reduction is the driving force towards particle coarsening and, thereby, to the progressive eradication of the nano-structure, undercutting the

* Corresponding author. Tel.: +972 8 6461472; fax: +972 6477148.
E-mail address: dariel@bgu.ac.il (M.P. Dariel).

0925-8388/$ – see front matter © 2012 Elsevier B.V. All rights reserved.
doi:10.1016/j.jallcom.2012.02.099

very reason for its presence. In addition to its formation, long term structural stability of a nanostructure is a necessary condition for its usefulness in conjunction with high thermoelectric energy conversion efficiency.

Among the Group IV–VI tellurides, PbTe and SnTe compounds have a rock salt cubic structure up to their melting point; the high temperature $GeTe_{\beta}$-phase undergoes on cooling at 700 K an allotropic transformation to rhombohedral $GeTe_{\alpha}$. In the pseudobinary (Ge,Sn)Te and (Sn,Pb)Te systems, complete mutual solubility prevails, while in the (Ge,Pb)Te system below 850 K a phase separation takes place into two Pb- and Ge-rich telluride compounds, respectively [3].

Recently Gorsse et al. [4] have studied the microstructural evolution induced by the phase separation that takes place in the course of aging at 500 °C in the pseudo-binary PbTe–GeTe system. Subsequently in a more extensive study, Gorsse et al. [5] identified in the initial stages of the phase separation a so-called "discontinuous spinodal decomposition" mechanism. The latter displays features associated both with a spinodal decomposition and with discontinuous precipitation. In particular they observed by electron microscopy an ultrafine lamellar nanostructure with 10–30 nm spacing and Energy dispersive spectroscopy (EDS) scan across the lamellae revealed continuous and complementary Pb and Ge composition modulations. The spinodal character of the phase decomposition is consistent with Volykhov et al. [3] conclusions regarding the binary (Pb,Ge)Te system. In conclusion, Gorsse et al. [5] concluded that even though the thermal conductivity decreased as a result of the decomposition reaction, this benefit was counterbalanced by an increased electrical conductivity. As a result, the thermoelectric quality factor of the (Pb,Ge)Te compound, as determined at the ambient temperature, did not change significantly.

The structural evolution in a pseudo-ternary (Pb,Sn,Ge)Te compound with low Sn content has been studied by Dado et al. [6,7], Gelbstein et al. [8,9]. The Sn cation has a size intermediate between those of Pb and Ge, its presence reduces the positive enthalpy arising from the size difference of the latter two cations. The addition of Sn to the pseudo-ternary $(Ge_xPb_{1-x})Te$ compounds lowers the maximum of the miscibility gap, or in other words, widens the domain of complete mutual solubility. Yashina et al. [10] reported that a spinodal decomposition takes place in $Pb_{1-x-y}Sn_yGe_xTe$ compounds for a Sn composition below $y = 0.3$. The spinodal decomposition is closely associated with the subsequent phase separation and the formation of a miscibility gap in the pseudo-ternary system. The demixing process that follows the spinodal decomposition gives rise to a two phase morphology on a submicron scale similar to that taking place in the pseudo-binary (Pb,Ge)Te system and has been studied for samples of composition $(Pb_{0.3}Sn_{0.1}Ge_{0.6})Te$ as a function of aging treatments at temperatures below the top of the miscibility gap. The highest temperature of the miscibility gap at this composition of the pseudo-ternary is located at approximately $x = 0.6$ Ge fraction of the cation concentration, at 590 °C.

A two-phase sub-micron structure evolves in the course of annealing treatments in the miscibility gap. This structure undergoes changes in the course of an annealing treatment. Some of the resulting microstructures are transitory; others display long term stability of the order of thousands of hours. It was of interest to determine the mechanism and kinetics of the separation processes that take place in the miscibility gap of the pseudo-ternary system. Such understanding in conjunction with the determination of the thermoelectric transport properties may allow inferring and optimizing the relationship that prevails between microstructure and the transport properties, relevant to thermoelectric conversion efficiency.

In the present study we have focused our attention on a sample with a significantly increased Sn content, $(Pb_{0.25}Sn_{0.25}Ge_{0.5})Te$ that lowered the top temperature of the miscibility gap. Preliminary investigation [9] has shown that this pseudo-ternary compound with the high Sn content displays a significantly higher figure of merit than that of its counterpart with lower Sn content. Actually this figure of merit, 1.18 at 450 °C, positions the compound among the most promising p-type available thermoelectric materials. It was of obvious interest to check whether this elevated figure of merit is maintained over lengthy operational durations that characterize functional thermoelectric materials.

The increased Sn composition, by decreasing the enthalpy term in the free energy available for the phase separation process, tends to suppress its initial spinodal decomposition stage. We shall describe the microstructural changes that take place in the course of the aging treatments. Subsequently, we shall report on thermoelectric transport properties changes which run in parallel with the microstructural evolution. The treatments and the transport properties measurements were carried out at temperatures that correspond to the temperature window of actual operation of thermoelectric materials. The results are meant to be useful for evaluating the stability of thermoelectric devices based on these materials.

2. Experimental procedures

The synthesis of the quaternary $(Pb_{0.25}Sn_{0.25}Ge_{0.5})Te$ compound was performed by melting the source materials (purity of 5N – Alfa Aesar) at appropriate concentrations under vacuum (10^{-5} Torr) in a rocking furnace at 1000 °C for 1 h followed by water quenching. The resulting ingot sample was solution treated under an argon atmosphere in a quartz tube at 600 °C for 96 h and quenched in ice water. The annealing temperature is in the single phase domain, above the maximum temperature of the two phase field. Small samples were cut from the initial homogenized ingot, sealed in Pyrex tubes under an argon atmosphere and aged at different temperatures (280 °C, 390 °C) for different durations of time. The heat treatments were performed in pyrex tubes which had been inserted into suitably sized holes drilled in a steel block that was placed in a furnace controlled to within ±2°. The aged samples were cold mounted in acrylic epoxy, polished to the 0.5 μm level and examined by scanning electron microscopy (Jeol-JSM 5600 SEM and Jeol-JSM 7400F HRSEM), high resolution transmission electron microscopy (Jeol-2010 HRTEM) and optical microscopy (Zeiss Axiovert 25). XRD analysis (Rigaku D/Max 2100, Cu-Kα) was performed after powdering the samples in a stainless steel mortar and pestle.

Thermal etching at 600 °C for 15 min under 10^{-5} Torr vacuum was performed after polishing the samples. HRTEM specimens were prepared by mounting the samples inside a copper tube (Ø = 3 mm) and mechanical polishing (Buehler Minimet polisher) to about 100 μm in thickness. Subsequent thinning was carried out with a dimple grinder (Gatan model 656) and a precision ion polishing system (Pips Gatan 691).A part of the initial solution treated ingot was comminuted by stainless steel ball milling to <60 mesh powder. The powder was subsequently consolidated by Spark Plasma Sintering (SPS) (type HP D 5/1 FCT Systeme GmbH) into disc shaped specimens. These were submitted to aging treatments similar to those undergone by the samples for structural evaluation. The thermal conductivity as a function of the temperature was performed by the flash diffusivity method (LFA 457, Netzsch). The thermal conductivity (κ) values were calculated using the equation $\kappa = \alpha\rho C_p$ where α is the thermal diffusivity, C_p is the specific heat (measured using differential scanning calorimetry, STA 449-Netzsch), and ρ is the bulk density of the sample.

3. Results and discussion

3.1. Microstructural evolution

The diffraction profile after the homogenization treatment in the single phase domain and quenching to room temperature is shown in Fig. 1. The agreement between the experimental spectrum and the theoretical pattern generated for a rhombohedral unit cell, as expected for the Ge-containing sample at room temperature, is excellent. The allotropic phase transformation in GeTe and in the $Pb_{1-x-y}Sn_yGe_xTe$ is believed to be a displacive phase transformation and the high temperature parent rock salt structure cannot be retained at the ambient temperature.

Scanning electron microscope (SEM) examination of all samples after a relatively short, 24 h, aging treatment at 280 °C after cooling from the high temperature single phase domain, revealed the appearance of a lamellar microstructure in some areas of the

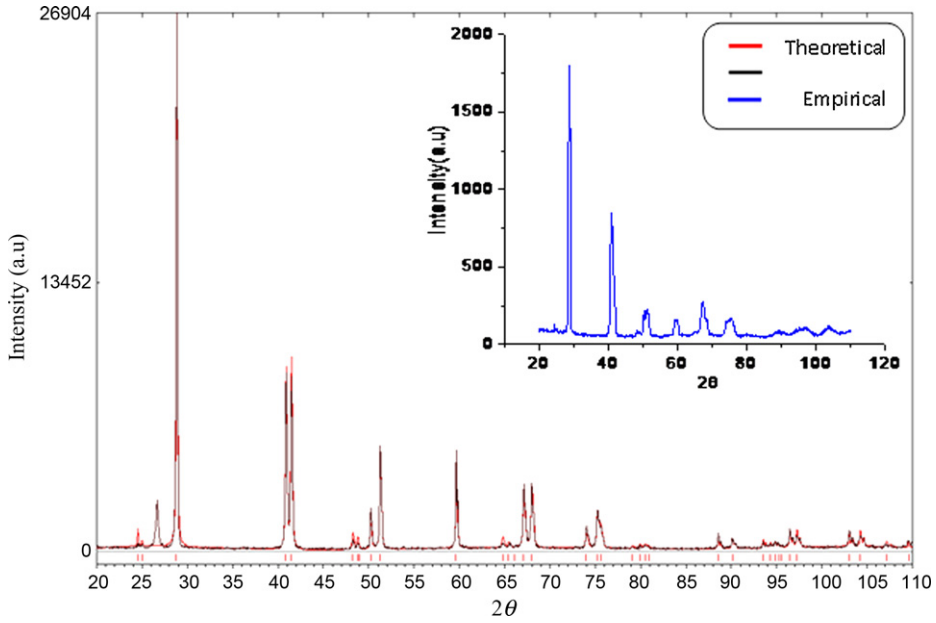

Fig. 1. Theoretical and experimental diffraction spectra after a 96 h solution treatment at 600 °C. The insert shows the spectrum after a short (30 min) solution treatment at 600 °C. The spectra correspond to the metastable rhombohedral Ge_{α} single phase structure at room temperature.

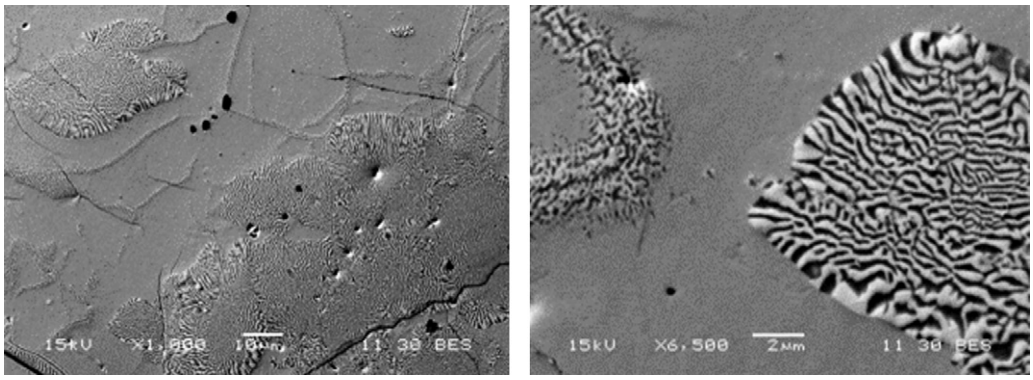

Fig. 2. SEM micrographs of a sample aged for 24 h at 280 °C. In (a) notice the preferential nucleation of the products of the cellular decomposition along the grain boundaries of the parent phase. In (b) at a higher magnification, notice the submicron structure of the discontinuous (cellular) decomposition. Notice also the orientation perpendicular to the decomposition front of the coupled components of the discontinuous precipitation.

specimen surface (Fig. 2). The lamellar microstructure consists of more or less parallel but non-straight, dark and bright lamellae and represents the product of the decomposition taking place at compositions within the miscibility gap. In the back-scattered electron (BSE) mode of the SEM examination, the bright areas are the heavy element (i.e. Pb) rich regions while the dark areas are the light element (i.e. Ge) rich areas. The lamellar microstructure suggests, in the absence of any other potential coupling microstructure mechanism, e.g. a eutectoid phase separation, that the phase separation in the course of the aging treatments took place via a discontinuous precipitation process.

This interpretation is fully supported by the diffractograms shown in Fig. 3, in which one discerns the appearance of two peaks at $2\theta = 28.5^{\circ}$ and 29.5°, respectively, even after the shortest aging treatment of 24 h at 390 °C, on both sides of the (0 1 2) diffraction peak of the rhombohedral phase into which the high temperature cubic phase transformed during or after cooling. These two low intensity and weakly resolved diffraction peaks stem from the appearance of the cellular decomposition products of the high temperature cubic phase, namely, a Pb-enriched phase with larger lattice parameter and a Ge-enriched phase with a smaller lattice parameter, respectively.

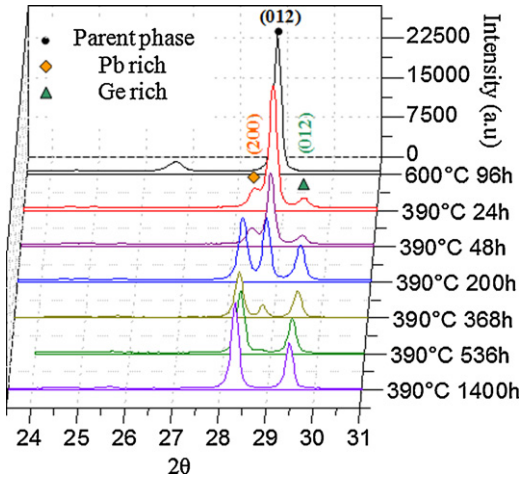

Fig. 3. Section 2θ, 28–31° of the diffraction spectra of a sample, initially solution treated at 600 °C and subsequently aged at 390 °C for different time durations. See the text for the details of the spectrum evolution process. The small and wide peak at 26.7° is due to carbon contamination in the SPS chamber.

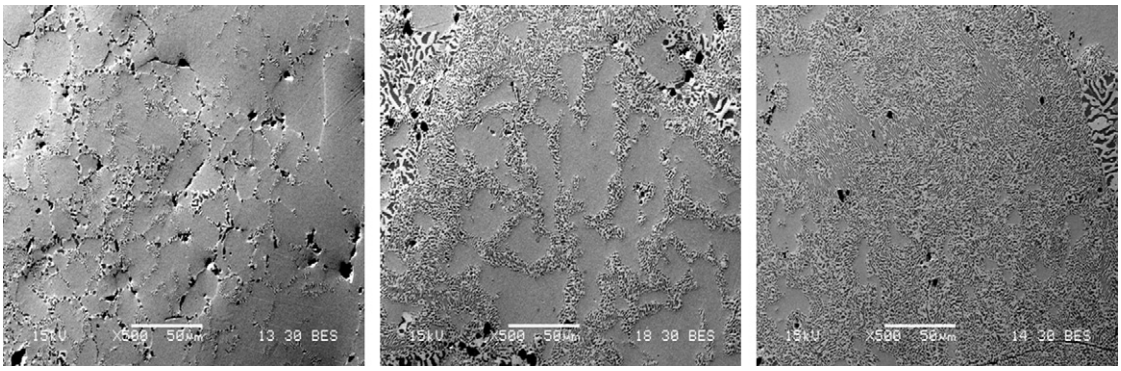

Fig. 4. ×500 micrographs of samples aged at 390 °C, (a) for 24 h, (b) 200 h, and (c) 368 h.

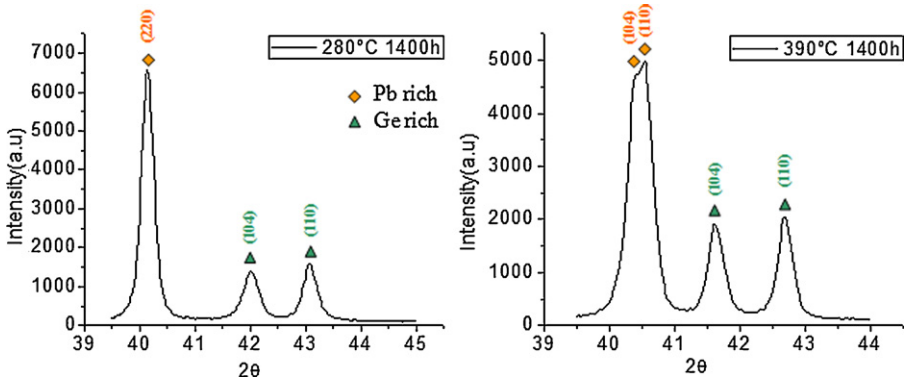

Fig. 5. Diffraction spectra sections of samples aged for 1400 h at (a) 280 °C, and (b) 390 °C.

The significant propensity of the initial nucleation stage to take place by heterogeneous nucleation anchored on grain boundaries, as evidenced in Fig. 2, underlines the reduced free energy available for the phase separation process in the relatively Sn-rich quasi-ternary compound. The heterogeneous nucleation process gives rise to the cellular (lamellar) structure, which is formed upon cooling the single phase (Pb,Sn,Ge)Te compound into the temperature range of the miscibility gap. The duplex coupled structure consists of alternate Pb-rich and Ge-rich isostructural telluride phases. This phase separation is identified as discontinuous precipitation because the initial composition of the high temperature single phase changes discontinuously upon crossing the interfaces to the newly formed Pb-rich and Ge-rich phases.

In the large smooth and featureless areas shown in Figs. 2 and 4, no apparent phase separation has yet taken place. The initial Ge concentration in the original compound implies however, that on cooling to the ambient temperature these areas have undergone an unavoidable structural transformation from the cubic rock salt Ge_β to the rhombohedral Ge_α structure. The subsequent discontinuous precipitation process by which the phase separation takes place can be expressed as:

$$(Pb, Sn, Ge)Te \rightarrow (Pb_R, Sn, Ge)Te + (Pb, Sn, Ge_R)$$

where $(Pb_R,Sn,Ge)Te$ and (Pb,Sn,Ge_R) stand for the Pb-rich and the Ge-rich rhombohedral phases bordering the miscibility gap, respectively.

With the elapse of aging time, increasingly larger fractions of the sample undergo the discontinuous precipitation process, as shown in Fig. 4 for the isothermal treatments carried out at 390 °C and supported by the diffraction spectra shown in Fig. 2.

In order to follow the kinetics of the phase separation process by discontinuous precipitation, the results of the XRD determinations were used in parallel with the results of the image analysis of the microstructure as a function of the aging duration. The results for aging treatment at 390 °C are summarized in Fig. 5

In the course of the cooling from the solution treatment at 600 °C and the subsequent aging treatment at 390 °C, two processes take place. The initial rock salt solid solution undergoes an allotropic transformation into the α-GeTe rhombohedral structure. In parallel phase separation starts to take place into a Pb-rich, $(Pb_R,Sn,Ge)Te$ phase, which reverts to the cubic structure (2 0 0) peak due to its low Ge content, and into the Ge-rich $(Pb,Sn,Ge_R)Te$ phase which retains the rhombohedral structure (0 1 2 peak). Whereas the structural transformation is very rapid and occurs in the (Pb,Sn,Ge)Te phase as long as the Ge/(Pb,Sn) ratio at ambient temperature does not fall below ≈0.3, the diffusion controlled phase separation process is significantly slower.

Even though most of the demixing process is completed in less than the first 368 h of the aging process, it may take much longer

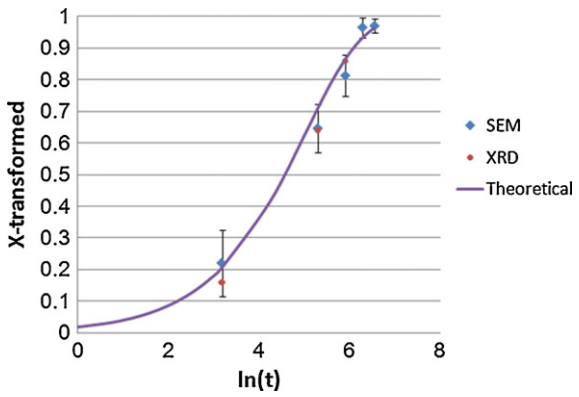

Fig. 6. JMA representation of the kinetics of the phase separation at 390 °C.

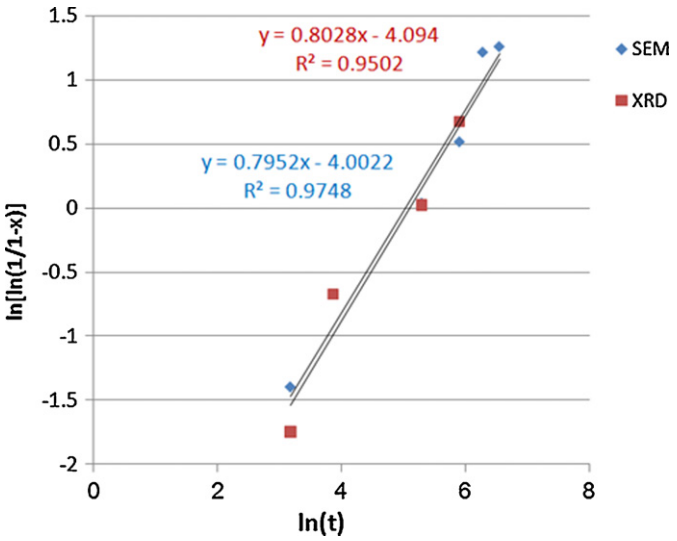

Fig. 7. Linearized JMA representation of the kinetics of phase separation at 390 °C.

to reach the thermodynamic equilibrium compositions of the two phases bordering the miscibility gap depending on the aging temperature, as evidenced in Fig. 5. The sections 2θ, 39–45° of the diffraction spectra of samples aged for 1400 h at (a) 280 °C and (b) at 390 °C are shown in Fig. 5. In both instances the phase separation in the miscibility gap was completed, leaving the two Pb- and Ge-rich phases, respectively, at their equilibrium composition. At the lower temperature, the Pb-rich decomposition product with a low Ge content has reverted to the cubic rock salt structure giving rise to the (2 2 0) diffraction peak. The Ge-rich component has undergone on cooling the transformation to the $GeTe_\alpha$ structure giving rise to the (1 0 4) and (1 1 0) diffraction peaks. At the higher (390 °C) aging temperature, the miscibility gap is narrower, composition-wise. The Pb-rich decomposition product has a higher Ge-content that at 280 °C and retains the original, high temperature Ge_β structure. At this low Ge content, the rhombohedral distortion of the cubic structure is very weak, as shown by the barely perceptible resolution of the initial (2 2 0) peak of the cubic structure into the rhombohedral (1 0 4) and (1 1 0) doublet (Fig. 5b).

The relative fraction $[1-Y(t)]$ that did not undergo two phase separation was determined and analyzed by an image processing software (Thixomat), for the aging treatments for different time durations at 390 °C. The time t dependence of the volume fraction transformed Y for a nucleation and growth dominated mechanism is described by the Johnson–Mehl–Avrami (JMA) equation,

$$Y(t) = 1 - \exp(-Kt^n) \quad (1)$$

where K is a temperature dependent parameter, which is constant for isothermal growth conditions, and n is the "shape factor," which depends on the growth dimension and is usually between 1 and 4. The dependence of Y on the aging time is shown in Fig. 6. Eq. (1) can be transformed to

$$\ln\left[ln\left(\frac{1}{1-Y}\right)\right] = \ln K + n \ln t \quad (2)$$

According to Eq. (2), a plot of $\ln(\ln(1/(1-Y))$ versus $\ln t$ should result in a straight line (Fig. 7) with a slope equal to that of the n. The shape factor n for the present study is 0.8, as shown in Fig. 7. The low value of n tends to indicate that the transformation is diffusion controlled. The value of n close to 1 suggests a transformation that was initiated mostly by grain boundary nucleation, in consistence with the micrographs shown in Fig. 2. The relatively good agreement of the experimental results with the JMA model supports the discontinuous precipitation model that is diffusion controlled.

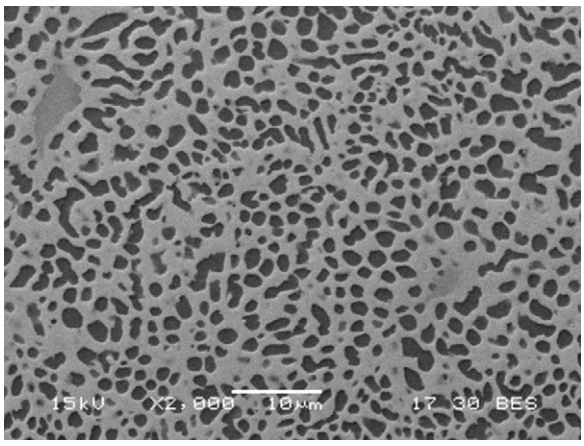

Fig. 8. ×2000 sample aged for 1400 h at 390 °C. The structure consists essentially of a Pb-rich matrix with embedded Ge-rich precipitates. Notice the smooth interface between precipitate and matrix.

Actually the diffusion that leads to phase separation is grain boundary diffusion at the front of the advancing coupled lamellae into the single phase region.

With further increase of the aging time, the lamellar duplex structure starts to break up and is gradually replaced by an increasingly spheroidized morphology, as shown in Fig. 8. The latter reflects the effect of reduction of the interface free energy. Some more subtle aspects of this process have been analyzed by Malzahn Kampe et al. [11].

Cellular or discontinuous precipitation has been studied extensively but mostly in metallic alloys. Much scarcer are reports on discontinuous precipitation in ceramic or semi-conductor material systems. Discontinuous precipitation displays several characteristic features that set it apart from the more conventional continuous precipitation process. Some of these features are clearly apparent in Fig. 9. First among these is the preferential nucleation of the two-phase structure adjacent to lattice discontinuities such as residual pores (A) and cracks (B). Preferential nucleation along grain boundaries also gives rise to the lack of microstructural symmetry along the two sides of a grain boundary (C). Discontinuous coarsening is apparent at (D). The perpendicular alignment of the lamellae to the phase separation front is clearly visible at (E). The sample in Fig. 9 had undergone a relatively advanced stage of decomposition after a lengthy aging treatment, as can be deduced from the areas in which

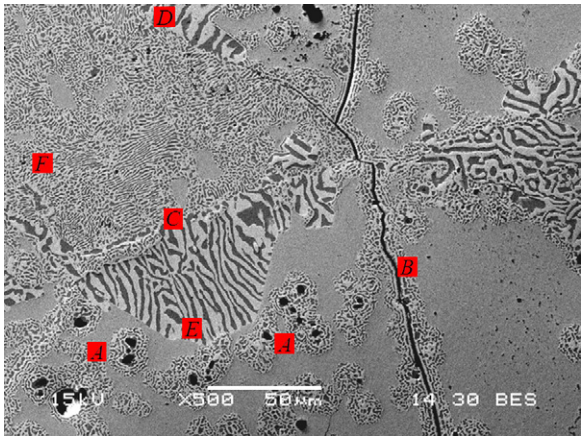

Fig. 9. Microstructure of a sample aged at 390 °C for 368 h. The micrograph puts in evidence several key characteristic features of the discontinuous precipitation process (see text).

Table 1
The composition of the various phases after the aging treatments at 390 °C.

	Pb (at%) ±1%	Sn (at%) ±1%	Ge (at%) ±1%	Te (at%) ±1%
Nominal composition	12.5	12.5	25	50
After quenching prior phase separation	12.8	14.5	19.4	54.2
Pb-rich phase				
Aging:				
24 h	20.6	16.7	12.2	50.4
48 h	20.8	15.6	12.0	51.6
200 h	20.0	17.1	11.9	51.0
368 h	21.6	18.7	10.4	49.7
1400 h	21.8	17.8	7.3	53.1
Ge-rich phase				
Aging:				
24 h	3.3	9.1	34.4	53.2
48 h	3.7	7.9	34.2	54.1
200 h	2.5	7.8	34.5	55.2
368 h	3.0	7.5	34.6	54.8
1400 h	3.3	8.3	34.1	54.3

the fine lamellar structure has broken down and started to undergo a spheroidization process (F).

From the microstructural features of Figs. 2a, b and 9, it appears that the transformation most often starts adjacent to lattice discontinuities such as grain boundaries or free surfaces. The vicinity of free surface alleviates the strain associated with the phase separation process and thereby favors the nucleation of the coupled lamellae.

The composition of the Pb- and Ge-rich phases after the decomposition process was checked by EDS measurements after the various aging treatments. The results along with the nominal composition and the composition of the as yet undecomposed solid solution after quenching are reported in Table 1. Several conclusions can be drawn from these experimental results:

a. The (Pb,Sn,Ge)Te system is properly speaking not a quasi-ternary system, it departs from this approximation at the high Ge concentration corner of the pseudo-ternary diagram.
b. The solubility of Ge in the Pb-rich telluride is significantly higher than that of Pb in the Ge-rich telluride. This observation accounts for the microstructure shown in Fig. 8, in which the Ge-rich precipitates (dark islands) are embedded in the majority Pb-rich (bright) matrix.
c. The solubility of Sn in the Pb-rich telluride is roughly twice as high as in the Ge-rich telluride, in consistency with the interaction parameters reported by Yashina et al.[10].

A transmission electron microscopy (TEM) image of the sample after a lengthy, 1400 h-long aging treatment at 390 °C, which has given rise to the spheroidized Ge-rich precipitates embedded in the Pb-rich matrix, is shown in Fig. 10. It shows two closely located Ge-rich precipitates, in which the parallel twin bands, generated in the course of the transformation from the high temperature cubic Ge_β to the rhombohedral Ge_α structure, are put in evidence. The two precipitates are interconnected by the Pb-rich matrix that has undergone during quenching a cubic to rhombohedral allotropic transformation, and subsequently, in the course of the phase separation, with the decreasing Ge content, reversion to the cubic rock salt structure of PbTe.

3.2. Thermoelectric transport properties

The thermoelectric transport properties and, in particular, the thermal conductivity, depend on various degrees of the microstructural changes and, thereby, affect the thermo-electric efficiency. It was of obvious interest to follow the inter-relationship between microstructure and thermoelectric properties in materials candidates for thermoelectric devices.

In order to examine the interdependence between the microstructural evolution and the thermoelectric transport properties, the Seebeck coefficient, the electrical and thermal conductivities, were determined as a function of temperature on samples that had undergone aging treatments for various time durations at 390 °C. The dependence of these properties on the duration of the aging treatment is shown in Fig. 11. The figure of merit of the thermoelectric materials ZT is expressed by $ZT = \beta^2\sigma/\kappa$ where β is the Seebeck coefficient, σ and κ, the electrical and thermal conductivities, respectively. The figure of merit is a measure of the material's efficiency in converting thermal to electric energy. In the course of the aging treatments that took place at a temperature within the miscibility gap in the pseudo-ternary diagram, the original single phase structure underwent a phase separation process. The very first data point in the three graphs (Fig. 11a–c) represents the values immediately after quenching from the high temperature single phase domain. At this point, most if not the entire sample, has not yet undergone any phase separation process. The subsequent data points reflect the values after the heat treatments. It is quite obvious that the most dramatic changes in all three transport properties take place in the course of the initial stages of the aging treatment. The temperature dependence of the thermal conductivity, as shown in Fig. 11, shows that the aged samples display a lower thermal conductivity than the initial single phase solution-treated and quenched sample. According to Gorsse et al. [4,5] the (Pb,Ge)Te sample aged for 1 min at 500 °C indeed displays a reduced thermal conductivity, but the reduction is short lived. After 10 min aging at 500 °C the thermal conductivity is already higher than in the as-quenched sample and increases substantially after longer aging treatments. The results regarding the electrical conductivity are also significantly different. The electrical conductivity of the Sn-free tellurides with respect to the as-quenched state increases continually with aging, whereas the Sn containing samples display a significant drop of the electrical conductivity following quenching. With increasing aging duration the electrical conductivity of the latter increases but still maintains values after 1400 h aging times that are below those of the as quenched single phase state. The Seebeck coefficient after an initial increase in the course of the shortest aging decreases slowly with increasing aging duration. In the present study the various transport properties of samples aged for different durations were measured as a function of the temperature; this allowed determining the temperature dependence of their figure of merit. The results indicate that the phase separation process that takes place in course of the aging treatment affects positively the figure of merit by approximately 20%, in contrast to Gorsse et al's conclusion according to which there is no improvement associated with the nano-patterning. Obviously the two studies dealt with samples having different composition and

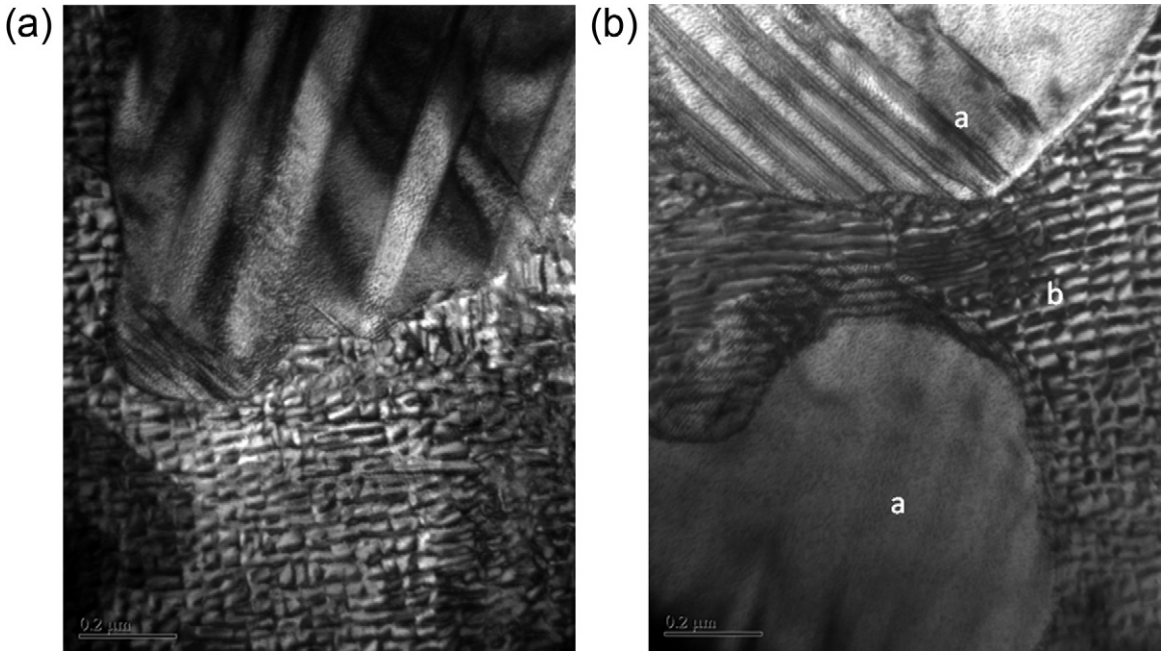

Fig. 10. TEM image of a sample aged at 390 °C for 1400 h, showing the Pb-rich matrix in which Ge-rich precipitates (a) are embedded. The parallel streaks in the precipitates are the twins generated in the course of the Ge_{β} to Ge_{α} allotropic transformation on cooling. The mottled aspect of the Pb-rich matrix (b) is due to the successive phase transformations that it had undergone. First, on quenching from the cubic structure at the homogenization treatment to the rhombohedral structure at room temperature, subsequently, after the phase separationand Ge depletion, reversion to the cubic structure.

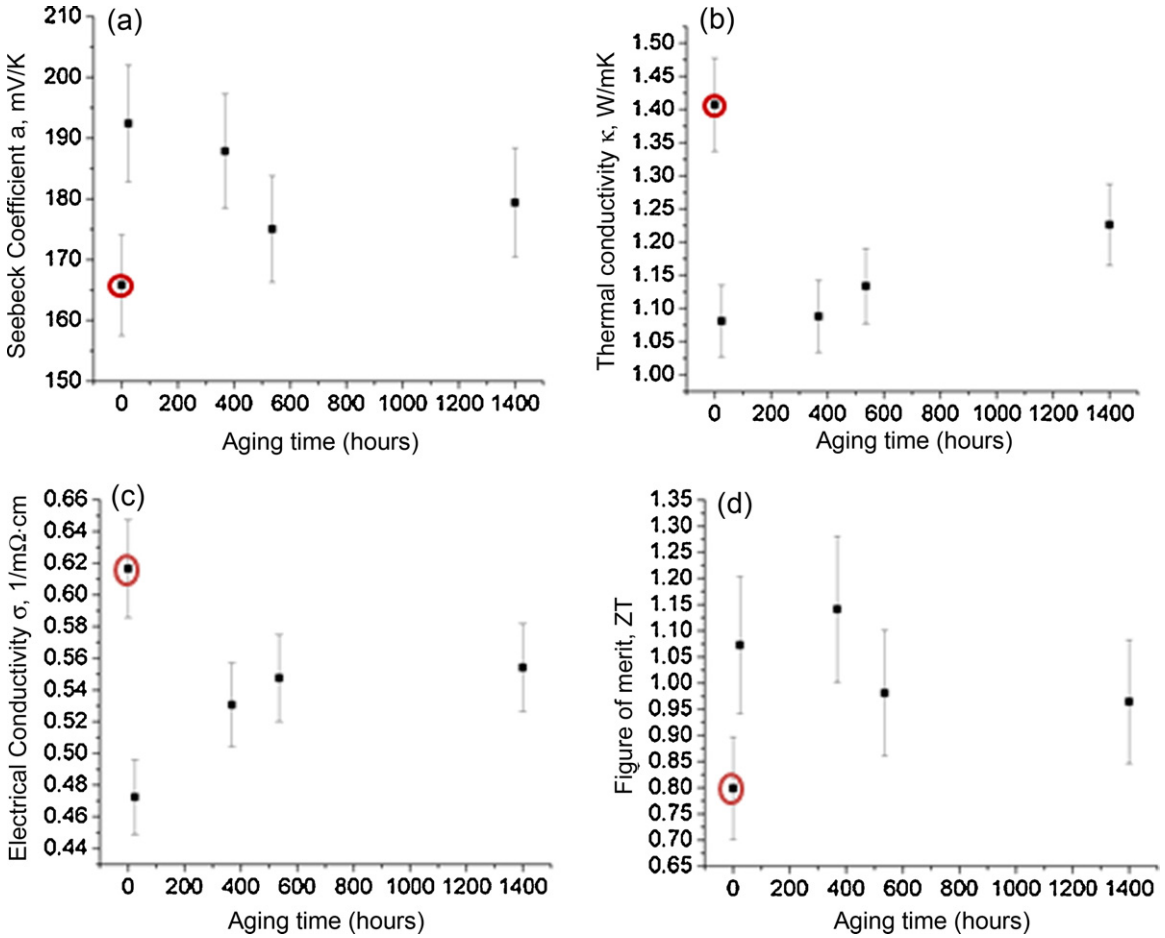

Fig. 11. The thermoelectric transport properties as a function of the aging duration at 390 °C after quenching from the single phase domain at 500 °C. (a) The Seebeck coefficient, (b) the thermal conductivity, (c) the electrical conductivity, and (d) the figure of merit, ZT. The first data point in each graph (circled) represents the value of the property in the as-quenched sample prior aging.

were aged at different temperature. Nonetheless, we believe that the subject is of sufficiently broad interest to warrant underlining their significantly different conclusions.

The aging treatments were carried out at 390 °C, a temperature which is located well within the interval of interest of high temperature reservoirs for conversion generators from waste heat in various industrial installations. The relatively high and long term stable value of the figure of merit of the p-type quasi-ternary compound, subject of the present study, offers the promise of its actual utilization as a viable thermoelectric material.

4. Conclusions

Following the spinodal decomposition in the quasi ternary $(Pb_{0.25}Sn_{0.25}Ge_{0.5})Te$ compound upon cooling from the high temperature single phase domain, phase separation takes place via a discontinuous precipitation process. The phase separation gives rise to two Pb- and Ge-rich tellurides, respectively.

The kinetics of phase separation was followed by microstructural image analysis and X-ray diffraction. The results showed good agreement with the Johnson–Mehl–Avrami model suggesting a diffusion controlled process initiated by grain boundary nucleation.

The initial lamellar structure of the two phases with interlamellar spacing ranging from 500 nm to 2 μm for aging treatment at 390 °C ranging from 30 min to 1400 h started to break up, generating a dispersion of 1–2 μm diameter spherical Ge-rich precipitates in a Pb-rich matrix.

The results of the phase separation regarding the composition, as determined by EDS measurements, were in good qualitative agreement with the quasi-ternary phase diagram and the interaction parameters published by Yashina et al. [10].

The thermoelectric transport property measurements (Seebeck coefficient, electrical and thermal conductivity), were carried out from room temperature to 500 °C. The results showed significant changes taking place in the initial stages of the aging treatments carried out at 390 °C. Even though the thermal conductivity value dropped significantly, its effect on the figure of merit was counterbalanced to a large extent by a parallel drop of the electrical conductivity. Nevertheless, the quasi-ternary compound, after an aging treatment of 1400 h, displayed a stable and the relatively high, for p-type compounds, figure merit value of 0.95 ± 0.07.

References

[1] T.T. Ikeda, V.A. Ravi, G.J. Snyder, Formation of Sb_2Te_3 Widmanstaetten precipitates in thermoelectric PbTe, Acta Mater. 57 (2009) 666–672.
[2] T.T. Ikeda, N.J. Marolf, K. Bergum, B.M.B. Toussaint, N.A. Heinz, V.A. Ravi, G.J. Snyder, Size control of Sb_2Te_3 Widmanstatten precipitates in thermoelectric PbTe, Acta Mater. 59 (2011) 2679–2692.
[3] A.A. Volykhov, L.V. Yashina, V.I. Shtanov, Phase equilibria in pseudoternary systems of IVVI compounds, Inorg. Mater. 42 (2006) 596–604.
[4] S. Gorsse, P. Bauer Pereira, R. Decourt, E. Sellier, Microstructure engineering design for thermoelectric materials: an approach to minimize thermal diffusivity, Chem. Mater. 22 (2010) 988–993.
[5] S. Gorsse, P. Bellanger, Y. Brechet, E. Sellier, A. Umarji, A. Alk, E. Decourt, Nanostructuration via solid state transformation as a strategy for improving the thermoelectric efficiency of PbTe alloys, Acta Mater. 59 (2011) 7425–7437.
[6] B. Dado, Y. Gelbstein, D. Mogyliansky, M.P. Dariel, Nucleation of nanosize particles following the spinodal decomposition in the pseudo-ternary (Ge0.6Pb0.3Sn0.1)Te compound, Scr. Mater. 62 (2009) 89–92.
[7] B. Dado, Y. Gelbstein, D. Mogyliansky, M.P. Dariel, Structural evolution following spinodal decomposition of the pseudoternary compound $(Ge_{0.6}Pb_{0.3}Sn_{0.1})Te$, J. Electron. Mater. 39 (2010) 2165–2171.
[8] Y. Gelbstein, Y. Rosenberg, Y. Sadia, M.P. Dariel, Thermoelectric properties evolution of spark plasma sintered $(Ge_{0.6}Pb_{0.3}Sn_{0.1})Te$ following a spinodal decomposition, J. Phys. Chem. C 114 (2010) 13126–13131.
[9] Y. Gelbstein, B. Dado, O. Ben-Yehuda, Y. Sadia, Z. Dashevsky, M.P. Dariel, High thermoelectric figure of merit and nanostructuring in bulk p-type $Ge_x(Sn_yPb_{1-y})_{1-x}Te$ alloys following a spinodal decomposition reaction, Chem. Mater. 22 (2010) 1054–1058.
[10] L.V. Yashina, V. Leute, V.I. Shtanov, H.M. Schmidtke, V.S. Neudachina, Phase relations in pseudobinary systems of germanium tin, and lead chalcogenides, J. Alloys Compd. 413 (2006) 133–143.
[11] J.C. Malzahn Kampe, T.H. Courtney, Y. Leng, Shape instabilities of plate-like structures—I. Experimental observations in heavily cold worked in situ composites, Acta Metall. 37 (1989) 1735–1745.